Iron Tris(bipyridine)-Centered Star Block Copolymers: Chelation of Triblock Macroligands Generated by ROP and ATRP

Robert M. Johnson[†] and Cassandra L. Fraser*

Department of Chemistry, University of Virginia, McCormick Road, P.O. Box 400319, Charlottesville, Virginia 22904-4319

Received October 3, 2003; Revised Manuscript Received January 6, 2004

ABSTRACT: A series of bipyridine (bpy)-centered triblock copolymers, BA-bpy-AB, were generated by ring-opening polymerization (ROP) and atom transfer radical polymerization (ATRP) mechanisms. Hydroxyl chain ends of poly(ϵ-caprolactone) (PCL) and poly(lactic acid) (PLA) precursors, $bpyPCL_2$ and $bpyPLA_2$, respectively, were converted to α-bromoesters for use as macroinitiators for the subsequent addition of second blocks, poly(methyl methacrylate) (PMMA) or poly(*tert*-butyl acrylate) (PtBA). Materials formed by sequential ATRP reactions, $bpy(PMMA\text{-}PS)_2$ and $bpy(PS\text{-}PMMA)_2$, were also produced. New $[Fe(bpy(AB)_2)_3]^{2+}$ analogues were formed by combination of triblock macroligands with $[Fe(OH_2)_6](BF_4)_2$ in 3:1 CH_2Cl_2:MeOH solutions. For $bpy(PCL\text{-}PtBA)_2$ and $bpy(PLA\text{-}PtBA)_2$ macroligands, only bis(bpy) materials resulted. Thermal properties of macroligands and iron(II)-centered polymers were investigated by differential scanning calorimetry (DSC) and thermogravimetric analysis (TGA). These synthetic studies lay the foundation for future investigations of how polymer composition and film morphology affect nanocluster formation in metal-centered star block copolymer templates.

Introduction

Block copolymers can form nanoscale assemblies in films[1−3] and solutions.[4−6] Selective introduction of metals into molecular and ensemble structures can lead to new kinds of functional materials with enhanced capabilities.[7−9] For example, metals serve as catalysts,[10] magnetic centers,[11−13] or optically active elements[14] in ordered films. In micelles, vesicles, and layered structures, metals are useful for detection.[15−17] In some cases, metals are integral parts of the polymer architecture, which determines their position in hierarchically structured assemblies. For example, controlled polymerization of metallomonomers can lead to metal-rich blocks[18] or even new kinds of nanoobjects upon postpolymerization processing.[19] Other times, when metal salts and other precursors are mixed with block copolymers, the metals segregate into one domain of the ordered material and not the other.[20,21] Alternatively, inorganic materials are added to preformed patterned substrates. Here, the block copolymer assembly serves as a template for selective small-scale metal patterning. In another powerful method, particular domains are etched or degraded,[22] and the resulting channels or voids can be backfilled with inorganic materials.[23−25] Though many of these methods for positioning metals on the nanometer scale are quite new, there have been significant advances in recent years, and existing methods continue to be improved.

Recently we reported on the serendipitous discovery of a new approach to inorganic−organic hybrid materials, wherein films of block copolymeric metal complexes serve as templates for metal-containing nanocluster formation.[26] Specifically, iron tris(bipyridine)-centered stars with poly(2-ethyl-*b*-2-undecyl)oxazoline (PEOX-*b*-PUOX) arms formed cylindrical morphologies when cast as films, with metal centers presumably distributed throughout the PEOX regions, as determined by their position at the core of star block copolymer structure. Upon annealing, iron-containing clusters ∼20−40 nm in size formed on the surfaces of the films, suggesting that the iron ions were released from the bipyridine binding sites and were reactive under these conditions. Though the patterning was not entirely uniform, particles were reasonably well distributed across the surface of the PEOX−PUOX film and showed some preference for the more polar PEOX domains. These initial observations have raised numerous questions about the roles of the metal center, polymer composition, block copolymer template morphology, and processing conditions on nanocluster formation. Greater understanding of this phenomenon in iron tris(bipyridine) polymers could ultimately be applied to other metals and materials with useful properties.

To understand the effects of polymer composition and morphology on nanocluster formation and to see whether greater positional control is possible, new kinds of iron-centered star block copolymers are required. Additionally, the bpy-centered triblock macroligands generated for polymeric metal complex (PMC) synthesis by chelation may be readily coordinated to other metals besides iron, too, to determine whether cluster formation is a general phenomenon. Here we report on the optimization of ring-opening polymerization (ROP) and atom transfer radical polymerization (ATRP) methods for generating new kinds of bpy-centered triblock copolymers comprised of poly(ϵ-caprolactone) (PCL), poly(lactic acid) (PLA), poly(methyl methacrylate) (PMMA), poly(*tert*-butyl acrylate) (PtBA), and polystyrene (PS) segments (Figure 1). Additionally, thermolysis of PtBA leads to poly(acrylic acid) (PAA) materials. The coordination of these macroligands to Fe(II) to generate star blocks and the thermal properties of these new materials are also described. Optimization of methods for generating bpy-centered triblock macroligands and their iron(II) complexes described herein lays the foundation for future investigations of how polymer composition and film morphology affect nanocluster formation in

* To whom correspondence should be addressed. E-mail: fraser@virginia.edu.

[†] Current address: The Lubrizol Corporation, Wickliffe, OH 44092.

10.1021/ma035494+ CCC: $27.50
Published on Web 03/19/2004

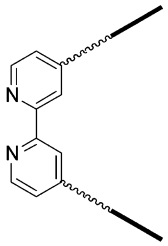

~~	———	#
PCL	PMMA	**4**
PCL	PtBA	**5a, 5b**
PLA	PMMA	**6**
PLA	PtBA	**7**
PS	PtBA	**8**
PS	PMMA	**9**
PMMA	PS	**10**

Figure 1. Schematic representation of the bipyridine-centered A−B−A triblock copolymers prepared via ROP−ATRP and ATRP−ATRP.

metal-centered star block copolymer templates. Additionally, systems containing biocompatible polyester segments are of potential interest as biomaterials with well-defined, cleavable metal coordinate cross-links.

Experimental Section

Materials. 4,4′-Bis(hydroxymethyl)-2,2′-bipyridine, bpy-$(CH_2OH)_2$, was synthesized as previously described.[27] ϵ-Caprolactone (Aldrich, 99+%), methyl methacrylate (Aldrich, 99%), and styrene (Aldrich, 99+%) were dried over CaH_2 and distilled under reduced pressure prior to use. *tert*-Butyl acrylate (tBA) (Aldrich, 98%) was washed with 5% NaOH (3×) and once with distilled H_2O, dried over $CaCl_2$, and distilled under reduced pressure. 3,6-Dimethyl-1,4-dioxane-2,5-dione (DL-lactide, Aldrich) was recrystallized (2×) from ethyl acetate and stored under nitrogen. Chloroform-*d* ($CDCl_3$) was passed through a short plug of dry, activated (Brockman I) basic alumina prior to use. Iron(II) tetrafluoroborate hexahydrate (Aldrich, 97%) was stored in a drybox and spectrophotometrically titrated using 2,2′-bipyridine (Aldrich, 99+%) and 4,4′-dimethyl-2,2′-bipyridine (GFS Chemicals) prior to use to verify the concentration of ferrous ions. Copper(I) bromide (Aldrich, 98%) and copper(I) chloride (Aldrich, 98%) were purified as previously described.[28] Toluene and tetrahydrofuran (Fisher) were purified by passage through alumina columns.[29] Triethylamine (Acros, 98.5%), 2-bromoisobutyryl bromide (Aldrich, 98%), tin(II) 2-ethylhexanoate ($Sn(Oct)_2$, Aldrich), and all other reagents were used as received.

Methods. ^{1}H NMR (300 MHz) spectra were recorded on a General Electric QE 300 spectrometer in $CDCl_3$. Resonances were referenced to the signal for residual protiochloroform at 7.260 ppm. ^{1}H NMR coupling constants are given in hertz. UV−vis spectra were obtained on a Hewlett-Packard 8452A diode-array spectrophotometer in CH_2Cl_2. Molecular weights were determined by gel permeation chromatography (GPC) ($CHCl_3$, 25 °C, 1.0 mL/min) using multiangle laser light scattering (MALLS) (λ = 633 nm, 25 °C), refractive index (λ = 633 nm, 40 °C), and diode-array UV−vis detection. A Polymer Labs 5μ "mixed C" guard column and two GPC columns along with Wyatt Technology Corp. (Optilab DSP interferometric refractometer, Dawn DSP Laser Photometer) and Hewlett-Packard instrumentation (series 1100 HPLC) and Wyatt Technology software (ASTRA) were used in GPC analysis. Incremental refractive indices (d*n*/d*c* values) for copolymers were estimated by a single injection method that assumed 100% mass recovery from the columns. Thermogravimetric analysis (TGA) was conducted using a TA Instruments TGA 2020 thermogravimetric analyzer over a temperature range from 30 °C to 500 °C with a heating/cooling rate of 10 °C/min under N_2. Differential scanning calorimetry (DSC) measurements were performed using a TA Instruments DSC 2920 modulated DSC, which was calibrated using an indium standard. Analyses were carried out in modulated mode under a nitrogen atmosphere (amplitude = ±1 °C; period = 60 s; heating rate = 5 °C/min; range −10 to 200 °C for **4**, **5**, and **7**, −10 to 300 °C for **6**, 50 to 300 °C for **8**−**10**). Reported values of thermal events are from the second heating cycle and the reversing heat flow curve unless indicated otherwise (T_g = midpoint of the change in heat capacity; T_d = onset point of decomposition). NOTE: Polymerizations were typically stopped prior to completion for increased molecular weight control. Reported yields are not corrected for incomplete monomer consumption.

Bpy(PCL-OC(O)C(CH$_3$)$_2$Br)$_2$, 1. A representative procedure for the synthesis of the 3° α-bromoester end-functionalized macroinitiator is as follows. A 25 mL round-bottom flask under N_2 was charged with bpyPCL_2 (0.408 g, 0.047 mmol, M_n = 8620, PDI = 1.07) and THF (5 mL), and the mixture was stirred until homogeneous. Triethylamine was added via syringe (55 μL, 0.39 mmol), the solution was stirred for 20 min and cooled to 0 °C, and 2-bromoisobutyryl bromide (35 μL, 0.28 mmol) was added dropwise. The reaction mixture slowly warmed to room temperature overnight (∼12 h) and subsequently was washed with a 1% (w/w) solution of $NaHCO_{3(aq)}$ (3 × 10 mL) and distilled water (10 mL). The organic layer was dried over Na_2SO_4 and filtered, and the solvent was removed in vacuo. The crude product was dissolved in CH_2Cl_2 (∼2 mL) and precipitated by dropwise addition to cold (−78 °C), stirring hexanes (40 mL). The mixture was centrifuged, the supernatant liquor was decanted, and the off-white solid was washed with additional hexanes (2×). The product was dried in vacuo to provide **1** as an off-white solid: 0.322 g (78%). ^{1}H NMR (300 MHz, $CDCl_3$): δ 8.67 (d, J = 5.0, H-6, H-6′), 8.38 (s, H-3, H-3′), 7.30 (d, J = 5.0, H-5, H-5′), 5.21 (s, bpyCH_2), 4.05 (t, J = 6.6, RCO_2CH_2), 2.30 (t, J = 7.3, CH_2CO_2R), 1.93 (s, CH_3), 1.63 (m, $COCH_2CH_2CH_2CH_2CH_2O$), 1.39 (m, $COCH_2CH_2CH_2CH_2CH_2O$).

Bpy(PLA-OC(O)C(CH$_3$)$_2$Br)$_2$, 2. Tertiary α-bromoester end-functionalized PLA was synthesized from bpyPLA_2 (M_n = 8208, PDI = 1.14) using the procedure described for **1** except that the crude product was precipitated from CH_2Cl_2/cold MeOH. The product was dried in vacuo to provide an off-white solid **2**: 0.253 g (63%). ^{1}H NMR (300 MHz, $CDCl_3$): δ 8.67 (d, J = 5.0, H-6, H-6′), 8.37 (s, H-3, H-3′), 7.28 (d, J = 5.0, H-5, H-5′), 5.10−5.32 (m, CH, bpyCH_2), 1.94 (s, C(Br)(CH_3)$_2$), 1.54−1.60 (m, CH_3).

Bpy(PCL-OC(O)CH(CH$_3$)Br)$_2$, 3. The 2° α-bromoester end-functionalized bpyPCL_2 was synthesized from bpyPCL_2 (M_n = 8896, PDI = 1.25) using the procedure described for **1**, except 2-bromopropionyl bromide was the acylating agent. The product, **3**, was dried in vacuo to provide an off-white solid: 0.330 g (82%). ^{1}H NMR (300 MHz, $CDCl_3$): δ 8.67 (d, J = 5.0, H-6, H-6′), 8.38 (s, H-3, H-3′), 7.30 (d, J = 5.1, H-5, H-5′), 5.21 (s, bpyCH_2), 4.05 (t, J = 6.6, RCO_2CH_2), 2.30 (t, J = 7.3, CH_2CO_2R), 1.82 (d, J = 6.9, H), 1.63 (m, $COCH_2CH_2CH_2CH_2CH_2O$), 1.39 (m, $COCH_2CH_2CH_2CH_2CH_2O$).

Bpy(PCL-PMMA)$_2$, 4. Representative procedure: In the N_2 drybox, a 10 mL flask was charged with CuBr (9.9 mg, 0.069 mmol), hexamethyltriethylenetetramine (HMTETA) (19 μL, 0.070 mmol), methyl methacrylate (0.689 g, 15.8 mmol), and anisole (1.50 mL) and was stirred until homogeneous (∼10 min). Then the bpy(PCL-OC(O)C(CH$_3$)$_2$Br)$_2$ macroinitiator, **1** (0.296 g, 0.034 mmol, M_n = 8750, PDI = 1.09), was added. Once all reagents were completely dissolved (∼5 min), the mixture was transferred to a Kontes flask. The flask was sealed, removed from the drybox, and placed in an 80 °C oil bath. The reaction was stirred for 120 min and then was quenched by immersion of the flask in ice water. The mixture was dissolved in THF and passed through a neutral alumina plug to remove the catalyst, and then the solution was concentrated in vacuo. The resulting polymer was precipitated from CH_2Cl_2/cold CH_3OH (2×), collected by centrifugation, and dried in vacuo to give **4** as a white solid: 0.840 g (85%). ^{1}H NMR (300 MHz, $CDCl_3$): δ 5.21 (s, bpyCH_2), 4.05 (t, J = 6.6,

RCO_2CH_2), 3.60 (s, PMMA-OCH_3), 2.30 (t, $J = 7.3$, CH_2CO_2R), 2.12−1.3 (complex m, PCL-CH_2 and PMMA CH_2), 1.2−0.7 (br m PMMA-CH_3). GPC: $M_n = 33\ 760$, $M_w = 38\ 180$, PDI = 1.13.

Bpy(PCL-OC(O)C(CH$_3$)$_2$-PtBA)$_2$, 5a. Representative procedure: In the drybox, a 10 mL Kontes flask was charged with $NiBr_2(PPh_3)_2$ (16.0 mg, 0.022 mmol), a $bpyPCL_2$ α-bromoester macroinitiator, **1** (99.9 mg, 0.011 mmol, $M_n = 9400$, PDI = 1.10), and toluene (1.4 mL). The mixture was stirred until homogeneous (∼10 min), and then tBA (0.467 g, 3.65 mmol) was added. The flask was sealed, removed from the glovebox, and placed in an oil bath at 90 °C for 48 h. The reaction was quenched by immersion of the flask in ice water. The mixture was then dissolved in THF and passed through a neutral alumina plug, concentrated in vacuo, and precipitated from THF into CH_3OH/H_2O (10:1 v/v) (3×). The mixture was centrifuged, and the solid was recovered by decanting the supernatant liquor and washing with additional cold methanol. After drying in vacuo, the product, **5a**, was obtained as a white solid: 0.198 g (35%). ^{1}H NMR (300 MHz, $CDCl_3$): δ 5.21 (s, $bpyCH_2$), 4.06 (t, $J = 6.6$, RCO_2CH_2), 2.30 (t, $J = 7.3$, CH_2CO_2R), 2.28−2.1 (br, CH_2CH(COOtBu), 1.63 (m, CH_2), 1.42 (s, $C(CH_3)_3$), 1.39 (m, CH_2). GPC: $M_n = 31\ 350$, $M_w = 33\ 110$, PDI = 1.06.

Bpy(PCL-OC(O)CH(CH$_3$)-PtBA)$_2$, 5b. The block copolymer macroligand, **5b**, was synthesized from the 2° bromoester-functionalized $bpyPCL_2$ (**3**) ($M_n = 9400$, PDI = 1.10) following the procedure outline for **5a**. The product was dried in vacuo to provide **5b** as a white solid: 0.224 g (57%). ^{1}H NMR (300 MHz, $CDCl_3$): δ 5.21 (s, $bpyCH_2$), 4.06 (t, $J = 6.6$, RCO_2CH_2), 2.30 (t, $J = 7.3$, CH_2CO_2R), 2.28−2.1 (br, CH_2CH(COOtBu), 1.63 (m, CH_2), 1.42 (s, $C(CH_3)_3$), 1.39 (m, CH_2). GPC: $M_n = 54\ 900$, $M_w = 57\ 948$, PDI = 1.06.

Bpy(PLA-PMMA)$_2$, 6. Representative procedure: The block copolymer macroligand bpy(PLA-PMMA)$_2$ was synthesized from the macroinitiator bpy(PLA-C(O)C(CH$_3$)$_2$Br)$_2$ (**2**) (0.102 g, 0.012 mmol, $M_n = 8500$, PDI = 1.14) and methyl methacrylate (1.16 g, 0.013 mol) with CuBr (18.4 mg, 0.186 mmol) and HMTETA (43.0 mg, 0.186 mmol) in anisole (1.24 mL) using the procedure described for bpy(PCL-PMMA)$_2$, except reactions were allowed to progress for ∼16 h. Purification and drying in vacuo provided **6** as a white solid: 0.677 g (54%). ^{1}H NMR (300 MHz, $CDCl_3$): δ 5.10−5.32 (m, CH, $bpyCH_2$), 3.60 (s, OCH_3), 1.90 (br CH_3), 1.81 (br, CH_2), 1.62−1.52 (m, CH_3, PLA), 1.02 (s, CH_3, PMMA), 0.84 (s, CH_3, PMMA). GPC: $M_n = 65\ 900$, $M_w = 82\ 200$, PDI = 1.25.

Bpy(PLA-PtBA)$_2$, 7. The bpy(PLA-PtBA)$_2$ macroligands were prepared from the bpy(PLA-C(O)C(CH$_3$)$_2$Br)$_2$ macroinitiator, **2** (25.1 mg, 0.003 mmol, $M_n = 6204$, PDI = 1.30), and *tert*-butyl acrylate (0.601 g, 4.69 mmol) with $NiBr_2(PPh_3)_2$ (6.0 mg, 0.008 mmol) in toluene (1.7 mL) following the procedure described for bpy(PCL-PtBA)$_2$. Purification and drying in vacuo yielded **7** as a white solid: 89 mg (14%). ^{1}H NMR (300 MHz, $CDCl_3$): δ 5.10−5.30 (m, CH, $bpyCH_2$), 2.29−2.1 (br, CH_2CH(COOtBu)) 1.95−1.74 (br, s, *meso* CH_2 of PtBA backbone), 1.68−1.24 (br, m, *meso* and *racemo* CH_2 of PtBA backbone, CH_3), 1.44 (s, $C(CH_3)_3$). GPC: $M_n = 31\ 540$, $M_w = 33\ 420$, PDI = 1.06.

Bpy(PS-PtBA)$_2$, 8. Representative procedure: In a drybox, CuBr (4.6 mg, 3.2 μmol) and HMTETA (9 μL, 3.3 μmol) were added to a 5 mL round-bottom flask and dissolved in acetone (0.5 mL). Once homogeneous (∼10 min), the bpy(PS-X)$_2$ (X = Cl or Br) macroinitiator (0.151 g, 0.015 mmol, M_n = 9.9 kDa) was added to the catalyst solution, and the mixture was stirred until homogeneous (∼20 min). The reaction mixture was charged with tBA (0.987 g, 7.7 mmol), and then the reaction flask was sealed and heated at 60 °C in an oil bath for ∼8 h. The reaction mixture was quenched by immersion of the flask in ice water. The resulting block copolymer was dissolved in CH_2Cl_2, filtered through a plug of neutral aluminum oxide, and concentrated in vacuo. The crude polymer residue was purified by precipitation from ethyl ether into 1:1 (v/v) cold methanol/water. The purified polymer was collected by centrifugation, washed with additional ice-cold methanol, decanted, and dried in vacuo to provide **9** as a white solid. Yield: 0.479 g (42%). ^{1}H NMR (300 MHz, $CDCl_3$): δ 7.2−6.9 (br, m, Ph), 6.7−6.3 (br, m, Ph), 2.3−2.1 (br, s, CH_2CH(COOtBu)), 1.9−1.48 (complex, m, CH_2, CH,), 1.43 (s, $OC(CH_3)_3$). GPC: $M_n = 43\ 830$, $M_w = 50\ 270$, PDI = 1.15.

Bpy(PS-PMMA)$_2$, 9. Representative procedure: In the drybox, a catalyst stock solution was prepared in a volumetric flask by combining CuBr (7.2 mg, 0.050 mmol), HMTETA (13 μL, 0.048 mmol), and anisole (5 mL). A 5 mL round-bottom was charged with the catalyst solution (1 mL, 0.010 mmol catalyst) and the bpy(PS-X)$_2$ (X = Cl or Br) macroinitiator (0.101 g, 0.010 mmol; $M_n = 8393$, PDI = 1.18), and the mixture was stirred until homogeneous (∼10 min). Methyl methacrylate (1.66 g, 0.017 mol) was added, and the solution was transferred to a Kontes flask, sealed, removed from the glovebox, and placed in an 80 °C oil bath. After stirring for approximately 16 h, the reaction was quenched by immersion of the flask in ice water. The crude material was dissolved in CH_2Cl_2, passed through a neutral alumina plug, and concentrated in vacuo. The polymer was further purified by precipitation from CH_2Cl_2/cold MeOH and dried in vacuo to provide **10** as a white powder: 0.938 g (53%). ^{1}H NMR (300 MHz, $CDCl_3$): δ 7.2−6.8 (complex m, Ph), 6.7−6.2 (complex m, Ph), 3.61 (s, OCH_3), 2.1−0.70 (complex m, PMMA: CH_3, CH_2; PS: CH_2). GPC: $M_n = 127\ 200$, $M_w = 170\ 300$, PDI = 1.34.

Bpy(PMMA-PS)$_2$, 10. Representative procedure: In the drybox, a 10 mL round-bottom flask was charged with CuCl (4.9 mg, 0.050 mmol), HMTETA (13.5 μL, 0.050 mmol), and toluene, and the mixture was stirred until homogeneous (∼10 min). Bpy(PMMA-X)$_2$ (X = Cl or Br) (0.101 g, $M_n = 15\ 230$, $M_w = 17\ 890$, PDI = 1.18) was added, and the mixture was stirred until it dissolved (∼10 min). Styrene (0.295 g, 2.85 mmol) was added, and the reaction was stirred until homogeneous (∼5 min). The mixture was transferred to a Kontes flask, and the flask was sealed, removed from the glovebox, and placed in a 110 °C oil bath. After stirring for 18 h, the reaction was quenched by immersion of the flask in cold water. The crude polymer was dissolved in CH_2Cl_2, passed through a neutral alumina plug, concentrated in vacuo, and further purified by precipitiation from CH_2Cl_2/cold CH_3OH (2×). The product was collected by centrifugation, the supernatant liquor was decanted, and the product was washed with ice cold CH_3OH. After drying in vacuo, **11** was obtained as a white powder: 0.287 g (72%). ^{1}H NMR (300 MHz, $CDCl_3$): δ 7.2−6.8 (br m, Ph), 6.7−6.2 (br m, Ph), 3.605 (s, OCH_3), 2.1−0.69 (complex m, PMMA: CH_3, CH_2; PS: CH_2). GPC: $M_n = 49\ 410$, $M_w = 68\ 510$, PDI = 1.38.

Representative Synthesis of Polymeric Iron(II) Complexes. A methanol stock solution of iron(II) tetrafluoroborate hexahydrate ($Fe(BF_4)_2 \cdot 6H_2O$) was prepared and spectrophotometrically titrated with 2,2′-dipyridyl prior to use in order to accurately determine the ferrous ion concentration. **[**Fe(bpyPS-PtBA$_2$)$_3$](BF$_4$)$_2$: A 1 cm path length cuvette was charged with 100 μL of iron stock solution (0.22 μmol). The iron solution was diluted to 625 μL with additional MeOH, and 3 equiv of bpy(PS-PtBA)$_2$ (28.7 mg, 0.66 μmol, M_n = 43 830) dissolved in CH_2Cl_2 (1.875 mL) were added (resultant solution 75% CH_2Cl_2/25% CH_3OH). The cuvette was sealed, and the reaction was stirred and monitored by UV−vis until a maximum absorbance was obtained (∼2 h). Polymeric metal complexes were purified as described for block copolymer macroligands For example, [Fe(bpyPS-PtBA$_2$)$_3$](BF$_4$)$_2$ was precipitated from CH_2Cl_2 into 1:1 CH_3OH/H_2O, collected, and dried in vacuo to provide a pink solid: 24.4 mg (85%). ^{1}H NMR (300 MHz, $CDCl_3$): δ 7.2−6.9 (br, m, Ph), 6.7−6.3 (br m, Ph), 2.3−2.1 (br s, CH_2CH(COOtBu)), 1.9−1.46 (complex m, CH_2, CH,), 1.44 (s, $OC(CH_3)_3$). UV−vis: λ_{max} MLCT = 530 nm; ϵ = 8972 M^{-1} cm^{-1}. Chelation efficiency[30] = 95%.

Results and Discussion

A. ROP−ATRP. 1. Macroligand Initiator Synthesis. Bipyridine-centered poly(lactic acid) (PLA) and poly(ϵ-caprolactone) (PCL) macroligands were synthesized by previously described procedures using $Sn(Oct)_2$ as the catalyst in bulk monomer at 130 and 110 °C, respec-

Scheme 1

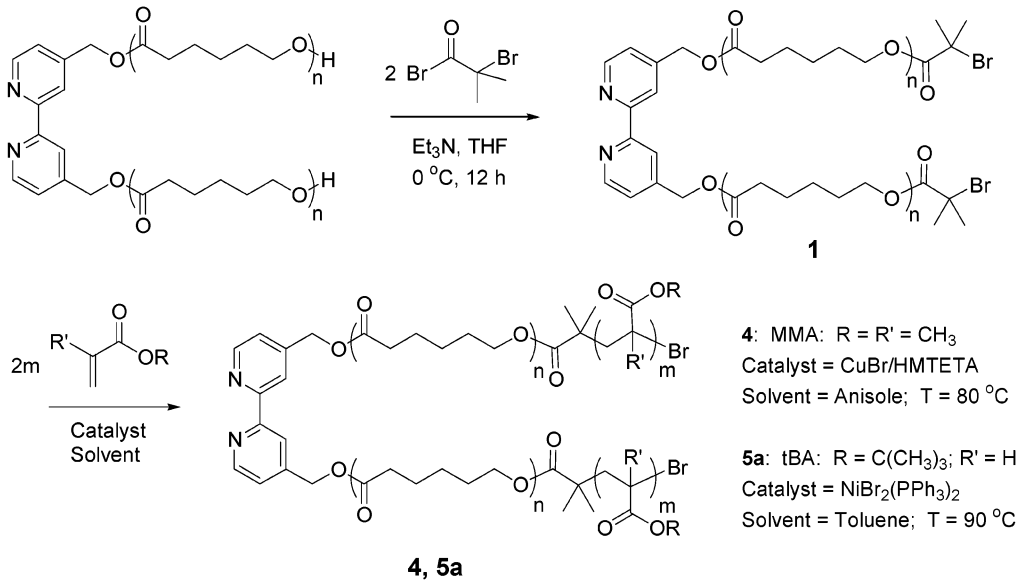

tively.[31] Macroligands were modified for use as initiators in the preparation of a second block via ATRP as illustrated in Scheme 1. Conversion of the alcohol end group to either a tertiary or secondary bromoester was carried out using excess 2-bromoisobutyryl bromide and 2-bromopropionyl bromide, respectively, in the presence of triethylamine to provide compounds **1**, **2**, and **3**. The formation of the ester functionality was confirmed by ^{1}H NMR through the disappearance of the protons associated with the methylene signal of the original end group (4.2 ppm) and the appearance of the signal from the methyl groups on the bromoester (1.93 ppm) (Figure 2). Yields for polymer products of the macroligand esterification reactions were typically >80% after purification by precipitation.

2. Preparation of Triblocks from ROP−ATRP. To design materials pertinent to biomedical applications such as drug delivery, we have prepared a series of block copolymer materials with biodegradable cores and biocompatible outer blocks. Extending our previous work with bpy-centered PLA and PCL homopolymers and block copolymers, here we combine ring-opening polymerization with atom transfer radical polymerization. Bromoester end-functionalized bpyPCL_2 and bpyPLA_2 were utilized as macroinitiators for the addition of a second block for the formation of bipyridine-centered ATRP−ROP−ATRP style triblocks. Bpy(PCL-PMMA)$_2$, **4**, was prepared from the tertiary bromoester-functionalized bpyPCL_2, **1**, in anisole using a CuBr/HMTETA catalyst system (Scheme 1). A 2:1 anisole:monomer ratio was employed in order to ensure complete macroinitiator dissolution.

A summary of GPC molecular weights for a variety of block sizes is provided in Table 1. Comparison of the GPC traces of the original macroinitiator and final triblock indicate the expected decrease in elution time with the addition of the methyl methacrylate block (Figure 3), with no change in the polydispersity (PDI). For further verification that the growth of the second block via ATRP was indeed controlled, the reactions were monitored over time, and the kinetics of polymer growth was determined to be first order with respect to monomer consumption (Figure 4). An M_n vs percent conversion plot exhibited linearly increasing molecular weights that paralleled calculated values, while polydispersities remained low (<1.3), consistent with a controlled or "living" process (Figure 5). Even at high conversion (>85%), the polymerization remained controlled, with only slight increases in the polydispersity, suggesting limited chain termination.

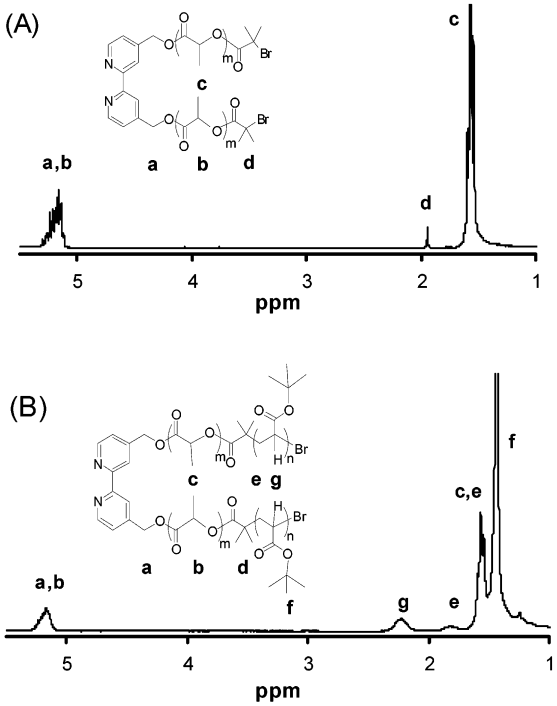

Figure 2. Comparison of ^{1}H NMR spectra ($CDCl_3$) of (A) a 3° α-bromoester end-functionalized bpyPLA_2 macroinitiator, **3,** and (B) a bpy(PLA-PtBA)$_2$ triblock, **7**.

Bpy(PLA-PMMA)$_2$ macroligands, **6**, were generated in a manner analogous to that for bpy(PCL-PMMA)$_2$ (i.e., a tertiary bromoester-functionalized bpyPLA_2 was used to initiate polymer growth with a CuBr/HMTETA catalyst system in anisole at 80 °C). Different block sizes were prepared for comparison (Table 1). Again, polydispersities remained low, consistent with a controlled polymerization. GPC analysis exhibited a decrease in retention time for the block copolymer relative to the original macroinitiator, corresponding to the increased molecular weight (Figure 6).

Table 1. Summary of GPC Molecular Weight Data for Representative ROP−ATRP Prepared Triblocks

	first block			triblock		
polymer	M_n[a] (kDa)	M_w (kDa)	PDI	M_n (kDa)	M_w (kDa)	PDI
bpy(PCL-PMMA)$_2$	11.7	12.4	1.07	33.8[b]	38.1	1.13
	23.0	25.0	1.08	83.2[c]	94.1	1.13
	23.0	25.0	1.08	53.0[d]	57.2	1.08
	32.0	34.5	1.08	174.4[e]	240.1	1.37
bpy(PLA-PMMA)$_2$	10.0	11.4	1.14	62.3[f]	75.2	1.21
	27.7	29.3	1.05	49.5[g]	62.4	1.26
bpy(PCL-PtBA)$_2$	9.4	11.6	1.10	54.9[h]	57.9	1.06
	9.4[i]	11.6	1.10	32.9[i]	36.6	1.11
bpy(PLA-PtBA)$_2$	27.8	33.0	1.11	42.2[j]	45.6	1.08
	6.2	8.1	1.30	32.5[k]	33.4	1.06

[a] Molecular weight determined using dn/dc = 0.056 mL/g (PCL) and 0.030 mL/g (PLA) in $CHCl_3$ using MALLS/RI detection. [b] MMA/catalyst/macroinitiator = 275:2:1; molecular weight estimated using dn/dc = 0.057 mL/g. [c] MMA/catalyst/macroinitiator = 745:2:1; dn/dc = 0.058 mL/g. [d] Polymerization stopped prior to completion; MMA/catalyst/macroinitiator = 900:2:1; dn/dc = 0.057 mL/g. [e] MMA/catalyst/macroinitiator = 1650:2:1; dn/dc = 0.059 mL/g. [f] Polymerization stopped prior to completion: MMA/catalyst/macroinitiator = 1000:2:1; dn/dc = 0.056 mL/g. [g] MMA/catalyst/macroinitiator = 200:2:1; dn/dc = 0.037 mL/g. [h] tBA/catalyst/macroinitiator = 350:2:1; dn/dc = 0.021 mL/g. [i] Initiator = 2° bromoester macroligand = bpy(PCL-OC(O)CH(CH_3)Br)$_2$; tBA/catalyst/macroinitiator = 206:2:1; dn/dc = 0.025 mL/g. [j] tBA/catalyst/macroinitiator 218:2:1; dn/dc = 0.026 mL/g. [k] tBA/catalyst/macroinitiator 220:2:1; dn/dc = 0.023 mL/g.

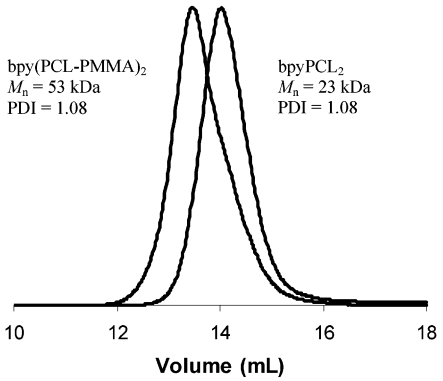

Figure 3. GPC overlay ($CHCl_3$) of bpy-centered poly(ϵ-caprolactone), bpyPCL$_2$, with the corresponding triblock bpy-(PCL-PMMA)$_2$.

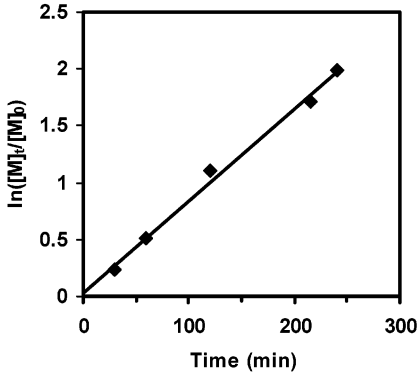

Figure 4. Kinetics plot for the polymerization of MMA from bpy(PCL-OC(O)C(CH_3)$_2$Br)$_2$ using the CuBr/HMTETA catalyst system in anisole at 80 °C (loading: monomer:catalyst:initiator = 1052:2:1).

Issues of catalyst, initiator, solvent, and monomer compatibility often arise in ATRP,[32] and this is clearly illustrated in the preparation of bpy(PCL-PtBA)$_2$ samples **5a** and **5b**. A variety of catalysts, solvents, and initiators

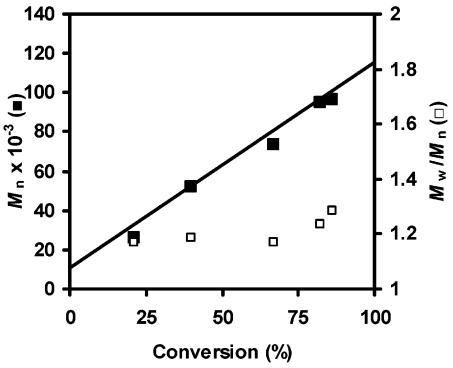

Figure 5. Number-average molecular weight (M_n) vs percent conversion plot for the generation of a bpy(PCL-PMMA)$_2$ triblock from bpy(PCL-OC(O)C(CH_3)$_2$Br)$_2$ using CuBr/HMTETA in anisole solution at 80 °C (— = M_n calcd) (loading: monomer:catalyst:initiator = 1052:2:1).

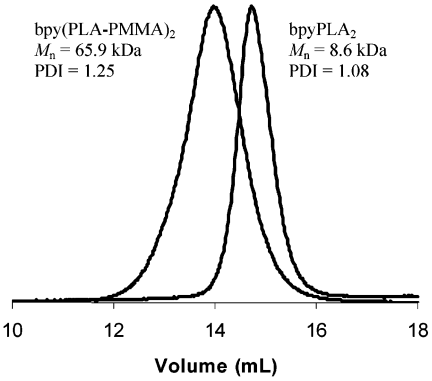

Figure 6. GPC overlay ($CHCl_3$) of a bpy-centered poly(lactic acid) bpyPLA$_2$ with the corresponding triblock bpy(PLA-PMMA)$_2$.

Table 2. Summary of Results from Screening Different Reaction Conditions for the Polymerization of *tert*-Butyl Acrylate from Bipyridine-Centered Poly(ϵ-caprolactone) Initiators

solvent	catalyst	initiator[a]	temp (°C)	result
acetone	CuBr/PMDETA	3°	60	no growth
anisole	CuBr/HMTETA	3°	60	no growth
anisole	CuCl/HMTETA	2°	60	no growth
bulk	CuBr/bpy$C_{13}H_{27}$	3°	110	poor control[b]
toluene	NiBr$_2$(PPh$_3$)$_2$	3°	90	controlled growth[c]
toluene	NiBr$_2$(PPh$_3$)$_2$	2°	90	controlled growth[c]

[a] Initiator: 3° = bpy(PCL-OC(O)C(CH_3)$_2$Br)$_2$, 2° = bpy(PCL-OC(O)CH(CH_3)Br)$_2$. [b] Poor control = multimodal GPC trace, PDI > 1.5. [c] Controlled growth = PDI < 1.3, unimodal GPC trace.

have been reported for the generation of linear polyacrylates via ATRP, and many of these were evaluated for compatibility with our system (Table 2). The first system explored for bipyridine-centered macroinitiators with a tertiary α-bromoester functional group was Cu(I)/HMTETA in anisole.[33] Though the copper(I) bromide/HMTETA catalyst has been used extensively for the ATRP of acrylates, with bpy(PCL-OC(O)C(CH_3)$_2$Br)$_2$ (**1**) as the macroinitiator, no PtBA growth was observed after 16 h. Because compatibility between the initiator and monomer may affect polymerization control, 2° α-bromoesters were also prepared from bpyPCL$_2$ for testing as macroinitiators. Again no PtBA growth was seen by GPC analysis after 16 h. We then turned to other known PtBA ATRP catalyst systems. Another common transition metal/ligand catalyst combination is Cu(I)/*N*,*N*′,*N*′,*N*″-pentamethyldiethylenetriamine (PM-

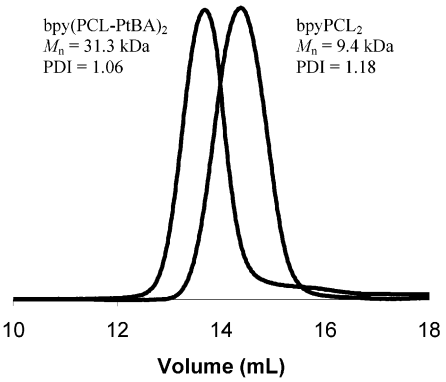

Figure 7. GPC overlay ($CHCl_3$) of a bpy-centered poly(ϵ-caprolactone), $bpyPCL_2$, with the corresponding triblock bpy-(PCL-PtBA)$_2$.

DETA).[34,35] Polymerization in acetone afforded no chain growth, as was evident by GPC analysis, probably due to the poor solubility of the $bpyPCL_2$ macroligand in acetone. Consequently, we focused on catalyst systems that were compatible with more suitable solvent systems for the polymer. Because copper catalysts have been successfully employed in ATRP reactions for the generation of bpy-centered macroligands, a Cu(I)/bpy-$(C_{13}H_{27})_2$ catalyst was evaluated.[36] The long alkyl chains solubilize the catalyst in toluene, which is a much better solvent for PCL. This combination resulted in polymer growth; however, GPC analysis indicated polymerization was uncontrolled as demonstrated by multimodal GPC traces, implying inefficient initiation or transesterification side reactions of the macroligand initiator during the course of the reaction. Polymerization of acrylates from a variety of initiators has been successful using $NiBr_2(PPh_3)_2$ in toluene solution,[37,38] and Wooley et al. have extended it to the generation of linear PCL-PtBA.[39] Controlled tBA polymerization was obtained for both initiators (**1** and **3**) in toluene solution at 110 °C after ~2 days. Materials with narrow molecular weight distributions were generated as shown in Figure 7.

Once conditions were established for the polymerization of *tert*-butyl acrylate from the $bpyPCL_2$ macroinitiator (**1**), this methodology was easily extended to the $bpyPLA_2$ system (**2**) as well. As with PCL, bpy(PLA-OC(O)C$(CH_3)_2$Br)$_2$ afforded triblocks with narrow molecular weight distributions (<1.1) using the $NiBr_2(PPh_3)_2$ catalyst in toluene at 110 °C (Table 1).

In contrast to the ^{1}H NMR spectra of the original PLA and PCL macroinitiators, the resonances due to bipyridine are not evident in the spectra for the ROP−ATRP block copolymer samples. This is similar to what has been observed previously for other bpy macroligands (e.g., polyoxazolines[40] and polystyrene[41]).

3. Preparation of Triblocks through ATRP−ATRP. Poly(styrene)-*b*-poly(methyl methacrylate) is among the most widely studied diblock copolymers for microphase separation and morphology studies.[42,43] Often it is prepared by anionic polymerization methods. The "living" nature of ATRP also lends itself to the preparation of diblock materials with narrow molecular weight distributions. Combining ATRP with coordination chemistry to generate well-defined polymeric architectures with labile metals as the central hub allows for the study of structural and compositional influences on microphase separation and the possibility of responsive materials that can change architecture by macroligand dissociation.

Diblocks may be generated via orthogonal or parallel mechanisms. For example, PS−PCL diblocks[44−46] including bipyridine-centered PS-bpy-PCL[47] have been synthesized from dual functional initiators by orthogonal ATRP and ROP polymerizations performed sequentially. In other cases, both blocks are formed by the same kind of (i.e., parallel) mechanism. For example, both PS and PMMA are formed by ATRP. In one strategy, the two sites of a dual functional initiator are sequentially activated for reaction. For example, in the synthesis of a PS-bpy-PMMA macroligand,[48] polystyrene was grown from a bpy(CH_2Cl) initiator site first, the "living" halide chain end was quenched, and then the second, previously dormant bpy(CH_2OH) site was activated as an α-bromoester initiator for polymerization of MMA. Alternatively, PS−PMMA diblocks may be prepared by sequential monomer addition to a "living" chain. For example, linear PS with halide chain ends prepared via living polymerization may be used as a macroinitiator for the ATRP of methyl methacrylate. Often, this is performed in a one-pot synthesis in which the second monomer is added prior to the consumption of the first[49] to avoid potential side reactions (e.g., termination, chain−chain coupling) often found at high monomer conversion. However, this results in tapered blocks (i.e., the first monomer is present in the second block), which may affect materials properties. Because of the stability of the chain end carbon−halide bond, it is also possible to grow the first block by ATRP, stop the reaction prior to the onset of side reactions, isolate and purify the resulting polymer, and then later resubmit it as a macroinitiator for the polymerization of the second block. However, the preparation of PMMA−PS and PS−PMMA diblocks with narrow molecular weight distributions (<1.3) is often difficult to achieve by this method due to differences in monomer activity and rates of cross-propagation.[50] These synthetic options provide routes to different polymer compositions and architectures.

For generating metal-centered star blocks, bpy-centered triblocks, PS−PMMA−PS, PMMA−PS−PMMA, and PtBA−PS−PtBA were targeted. Halide-terminated $bpyPMMA_2$ was used as a macroinitiator for polymerization of styrene second blocks.[51] The reaction to form $bpyPMMA_2$ was quenched in an ice water bath prior to complete monomer conversion (60−80% conversion) in order to minimize premature termination or side reactions due to chain−chain coupling at low monomer concentration. The resulting PMMA macroinitiator was purified by passage through a neutral alumina plug to remove the catalyst, followed by precipitation (2×) from CH_2Cl_2/CH_3OH. Polymerization of styrene from the $bpyPMMA_2$ macroligand was performed using a mixed halide system[52] in which the living chain ends of the macroinitiator were bromides and the catalyst employed was CuCl. The molecular weight distributions of the resulting PS−PMMA−PS materials were relatively broad (PDI ~1.4) (Table 3), as has also been observed by other groups for related systems.[53,54]

The synthesis of PS−PMMA copolymers, in which PMMA is grown second, is not as straightforward as other block preparations. Controlled chain extension requires that the rate of cross-propagation be equal to or greater than the rate of subsequent monomer addition. If this is not the case, some initiator sites will extend rapidly, while others do not, which can sometimes result in bimodal (or multimodal) molecular

Table 3. GPC Molecular Weight Data for Representative ATRP−ATRP Triblocks

	first block			triblock		
polymer	M_n (kDa)[a]	M_w (kDa)	PDI	M_n (kDa)[b]	M_w (kDa)	PDI
bpy(PS-PMMA)$_2$	25.4	27.6	1.09	55.5[c]	75.1	1.35
	8.4	10.0	1.18	127.2[d]	170.3	1.34
bpy(PS-PtBA)$_2$	16.4	18.8	1.14	64.5[e]	69.1	1.07
	9.9	11.8	1.09	43.8[f]	50.3	1.14
	23.6	28.7	1.22	31.8[g]	37.8	1.19
bpy(PMMA-PS)$_2$	15.2	17.9	1.18	58.2[h]	80.8	1.38

[a] Molecular weight determined using dn/dc = 0.145 mL/g (PS) and 0.059 (PMMA) in $CHCl_3$ using MALLS/RI detection. [b] Molecular weights determined using one-shot dn/dc measurements in which 100% mass recovery from columns was assumed. [c] MMA:catalyst:macroinitiator = 450:2:1 dn/dc = 0.098 mL/g. [d] MMA:catalyst:macroinitiator = 1635:2:1 dn/dc = 0.065 mL/g. [e] tBA:catalyst:macroinitiator = 403:2:1; dn/dc = 0.046 mL/g. [f] tBA:catalyst:macroinitiator = 280:2:1 dn/dc = 0.045 mL/g. [g] tBA:catalyst:initiator 100:2:1; dn/dc = 0.111 mL/g. [h] PS:catalyst:macroinitiator = 650:2:1; dn/dc = 0.123 mL/g.

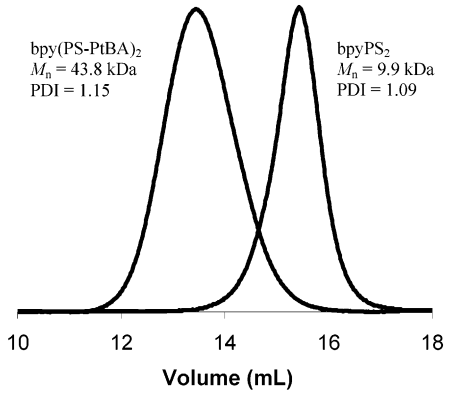

Figure 8. GPC overlay ($CHCl_3$) of a bpy-centered polystyrene bpyPS_2 with the corresponding bpy(PS-PtBA)$_2$ triblock.

weight distributions.[55] Matyjaszewski has shown that the inefficient initiation of methyl methacrylate from a secondary halide may be overcome in some cases by the use of halide exchange to affect the rate of cross-propagation.[50] To test this with our system, halide-terminated polystyrene was prepared and purified as previously described.[56] The active carbon−halide bond was exploited for the addition of MMA and tBA.

In reactions involving bpyPS_2 macroinitiators, a shoulder is typically observed, indicative of slow cross-propagation. The use of a CuCl catalyst with a Br end-capped PS did not efficiently initiate growth of poly(methyl methacrylate) but did result in a reduced concentration of the unreacted macroinitiator compared to reactions using the CuBr system. Preparative GPC could be used to separate the block copolymer from the unreacted macroinitiator if desired. Molecular weight distributions remained moderate (∼1.35) even at high molecular weights (>100 kDa).

The application of ATRP for the preparation of polystyrene-poly(*tert*-butyl acrylate) diblocks is well established.[57,58] For the generation of PS−PtBA (Scheme 2), the rate of cross-propagation is rapid compared to chain addition, thus resulting in controlled growth of the second block.[52] Bpy(PS−PtBA)$_2$ macroligands were prepared by known methods using CuBr/HMTETA and CuBr/PMDETA in acetone with varying block sizes (Table 3). Polymers were purified by precipitation from ethyl ether into 1:1 cold methanol/water. Comparison of the GPC trace of the triblock to that of the original

Scheme 2

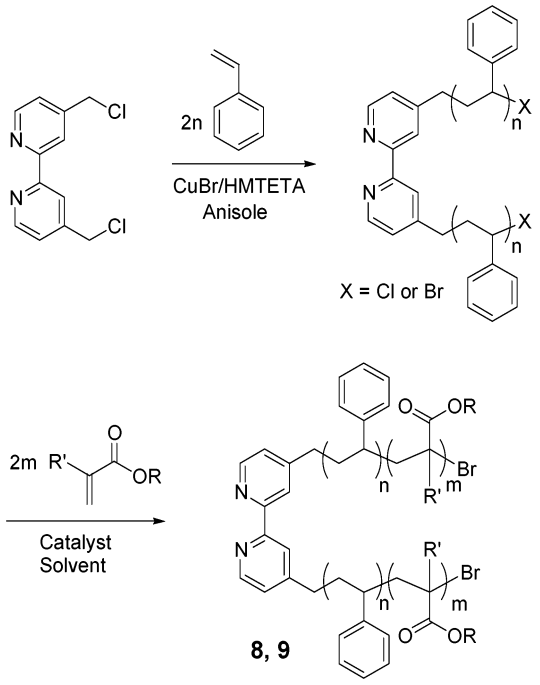

8: tBA: R = $C(CH_3)_3$, R' = H; Catalyst = $NiBr_2(PPh_3)_2$; Solvent = Toluene; T = 60 °C

9: MMA: R = R' = CH_3; Catalyst = CuBr/HMTETA; Solvent = Anisole; T = 80 °C

macroinitiator shows the expected shift in the elution volume, indicative of an increase in molecular weight (Figure 8). Again, polydispersities remain low (<1.2) for most reactions.

4. Chelation of Bipyridine-Centered B−A−B Triblocks to Iron(II). Iron(II) tris(bipyridine)-centered star block copolymers were generated by combining macroligands with $Fe(BF_4)_2{\cdot}(H_2O)_6$ (eq 1). To maximize

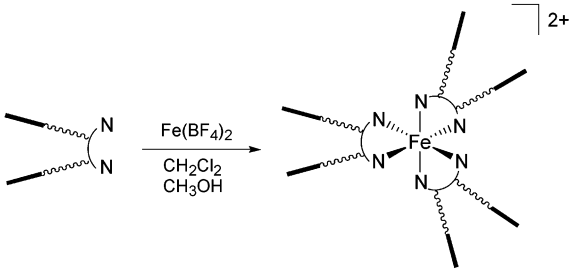

(1)

formation of the polymeric metal complex, careful consideration of the reaction conditions is required. Iron(II) salts require polar solvents like water or methanol, while most polymeric ligands in the triblock materials set (Figure 1) favor less polar media like tetrahydrofuran or chloroform. Additionally, the metal complex may be unstable in certain solvents. For example, iron(II) tris(bipyridine)-centered star polymers have been shown to dissociate ligands in the presence of acid or peroxides, such as those that form in chloroform or tetrahydrofuran.[31] Careful balancing of the requirements of the metal salt, the polymeric ligand, and the final complex and the desire for relatively consistent methods so that comparisons can be made between different macroligands led us to a mixed solvent system comprised of

Table 4. Summary of UV−Vis Data of Iron-Centered Star Block Copolymers

$[Fe(bpyX_2)_3](BF_4)_2$[a]	M_n(calcd) (kDa)[b]	ϵ_{PMC} (M^{-1} cm^{-1})[c]	time (min)[d]	chelation efficiency[e]
$[Fe(bpy(PCL\text{-}PMMA)_2)_3]^{2+}$	60.4	9375	28	0.99
	114.8	5900	60	0.62
$[Fe(bpy(PLA\text{-}PMMA)_2)_3]^{2+}$	60.1	9423	25	1.00
	149.0	7413	60	0.78
$[Fe(bpy(PS\text{-}PtBA)_2)_3]^{2+}$	76.0	9500	23	1.00
	131.7	8972	75	0.95
$[Fe(bpy(PS\text{-}PMMA)_2)_3]^{2+}$	221.6	6835	185	0.72
$[Fe(bpy(PMMA\text{-}PS)_2)_3]^{2+}$	174.8	8708	55	0.92

[a] Complexes prepared in 3:1 CH_2Cl_2/CH_3OH and monitored by UV−vis until the absorbance reached a maximum and remained constant. [b] Calculated molecular weight of the complex (determined from macroligand GPC molecular weight data) including associated BF_4^- counterions. [c] Molar absorptivity calculated from the maximum absorbance of the MLCT band (λ_{max} = 530 nm) obtained after stirring 3:1 macroligand:Fe $(BF_4)_2$. [d] Time to reach maximum absorbance. [e] The estimated chelation efficiency: $\epsilon_{MLCT}[Fe(bpyX_2)_3]^{2+}/\epsilon_{MLCT}[Fe(bpy)_3]^{2+}$. $\lambda_{max}[Fe(bpy)_3]^{2+}$ in 3:1 CH_2Cl_2/CH_3OH = 522 nm, ϵ = 9450 M^{-1} cm^{-1}.

75% dichloromethane and 25% methanol. Higher percentages of methanol resulted in cloudy solutions for certain high molecular weight macroligands (e.g., PS and PMMA > ∼45 kDa).

To accurately assess product formation in reactions of polymeric macroligands with the ferrous ion, chelations were performed in a sealed 1 cm path length cuvette and absorbances were monitored over time until a maximum value was reached. First, the ferrous ion concentration for a stock solution of $Fe(BF_4)_2 \cdot 6H_2O$ was determined spectrophotometrically using 2,2′-bipyridine and was further verified with 4,4′-dimethyl-2,2′-bipyridine. Once an accurate Fe(II) concentration was determined, an aliquot (100 μL) was added to a cuvette and diluted to 625 μL. A dichloromethane solution of the macroligand (1.875 mL) was added, resulting in a 75% CH_2Cl_2/25% CH_3OH reaction solution. The cuvette was sealed and the contents were stirred, with absorbances recorded at regular intervals (∼5 min) to monitor formation of the tris polymeric complex (λ_{max} = 530 nm). Once a maximum value was reached, the extinction coefficients were calculated. Chelation efficiency (CE) refers to the ratio of the extinction coefficient determined from λ_{max} for the polymeric metal complex with that of $[Fe(bpy)_3](BF_4)_2$ (ϵ_{bpy}; λ_{max} = 522 nm). These data are summarized in Table 4. Previous findings with homopolymeric iron(II) tris(bpy) complexes indicate that extinction coefficients for polymeric metal complexes (ϵ_{pmc}) are comparable to that of $[Fe(bpy)_3](BF_4)_2$ (ϵ_{bpy}); ϵ_{pmc} values vary little with polymer composition for reactions that proceed to completion.[59] Thus, we assume that chelation efficiency, $\epsilon_{pmc}/\epsilon_{bpy}$, is a good estimate of the extent to which an Fe tris(bpy) coordination reaction proceeded.

Chelation efficiencies for triblocks varied depending upon polymer molecular weight and composition. As is illustrated in Table 4, most macroligands form tris complexes efficiently (CE ∼ 0.95−1.00) for lower molecular weights (∼20−25 kDa); however, CEs begin to drop off as the molecular weights increase (e.g., $[Fe\{bpy(PCL\text{-}PMMA)_2\}_3]$: M_n(calcd) = 60.4 kDa, nearly quantitative polymeric complex formation; M_n(calcd) = 115K, 62% tris product formation). The molecular weight range for which efficiency drops is polymer dependent. For example, the PS−PtBA system forms tris product reasonably well at M_n = 131.7 kDa (CE = 0.95), whereas a 114.8 kDa PCL−PMMA macroligand has already dropped to CE = 0.62. Additionally, if a polymeric macroligand is of sufficiently high molecular weight, binding of a third macroligand may be slow or even prevented. A monobipyridyl ferrous complex forms immediately with $bpy(PLA\text{−}PMMA)_2$ (M_n = 62 kDa), then the equilibrium gradually shifts to a bis complex after ∼30 min, and finally, after ∼12 h, a small amount of tris complex is generated (CE = 0.15).[60] Even more dramatically, only iron bis(bpy) complexes (λ_{max} = 304 nm) were observed for $bpy(PCL\text{-}PtBA)_2$ (M_n = 32.9 kDa; PCL = 9.4 kDa) and $bpy(PLA\text{-}PtBA)_2$ (M_n = 42.2 kDa; PLA = 27.8 kDa).[60] This implies a much lower molecular weight threshold for these polyesters relative to other triblocks that were investigated. The reasons for these differences among polymers may stem from variations in chain conformation in the 3:1 CH_2Cl_2:CH_3OH solvent system and steric hindrance surrounding the metal binding site. Energetic preferences of polymer−polymer vs polymer−solvent interactions also play a role. Tris(bpy) complexes may still be possible for lower molecular weights of these polyester materials. Molecular weights where efficiency begins to drop for a given polymer are also undoubtedly solvent dependent.

Table 5. Thermal Analysis Data for Bipyridyl-Centered A−B−A Triblock Copolymers

macroligand	M_n (kDa)[a] first block	M_n (kDa)[a] triblock	T_g[b] (°C)	T_d[c] (°C)
$bpy(PCL\text{-}PtBA)_2$	9.2	32.9	46	195/295[d]
$bpy(PCL\text{-}PMMA)_2$	25.0	53.0	124	282
$bpy(PLA\text{-}PMMA)_2$	27.7	49.5	102	302
$bpy(PLA\text{-}PtBA)_2$	29.4	36.6	49	215/305[d]
$bpy(PS\text{−}PtBA)_2$	9.9	43.8	109	205/321[d]
$bpy(PS\text{−}PMMA)_2$	8.4	127.0	126	309
$bpy(PMMA\text{-}PS)_2$	20.4	58.2	99/127	316

[a] Determined by MALLS using d*n*/d*c* values provided in Tables 1 and 2. [b] Determined from the midpoint of the change in heat capacity. [c] The onset temperature for the decomposition as determined by TGA. [d] The first T_d corresponds to the thermolysis of *tert*-butyl groups.

B. Thermal Properties of Bpy-Centered Triblocks and Polymeric Metal Complexes. Modulated DSC and TGA analyses were performed to further characterize the bipyridine-centered ligands and resultant polymeric metal complexes. Summaries of the thermal analysis of the diblocks and polymeric metal complexes are provided in Tables 5 and 6, respectively. Block copolymers comprised of polystyrene and poly(methyl methacrylate) exhibited the expected glass transition temperatures (T_g) at ∼ 99 and 126 °C, respectively, reflective of the immiscibility of the two phases. For samples in which one block was significantly larger than another, typically only the T_g corresponding to the majority block was observed. DSC analysis of polymers with *tert*-butyl acrylate exhibited an endothermic event in the first heating cycle corresponding to the decomposition of the *tert*-butyl groups resulting in the conversion to poly(acrylic acid) at ∼220 °C. This was further verified by TGA, from which a distinct decomposition was observed at ∼210 °C. The loss of mass directly corresponded to the loss of isobutene due

Table 6. Thermal Analysis Data for Fe-Centered Polymeric Metal Complexes Prepared from Bipyridyl-Centered A−B−A Triblock Copolymers

iron complex[a]	M_n(calcd) (kDa)[b]	T_g[c] (°C)	T_d[e] (°C)
$[Fe(bpy(PCL\text{-}PMMA)_2)_3]^{2+}$	159.2	126	290
$[Fe(bpy(PLA\text{-}PMMA)_2)_3]^{2+}$	149.0	102	304
$[Fe(bpy(PS\text{-}PtBA)_2)_3]^{2+}$	131.7	108	201/300[e]
$[Fe(bpy(PS\text{-}PMMA)_2)_3]^{2+}$	221.6	122	307
$[Fe(bpy(PMMA\text{-}PS)_2)_3]^{2+}$	174.8	99/126	319

[a] Iron complexes generated from bpy-centered triblocks given in Table 5. [b] Calculated molecular weight of the complex determined from macroligand GPC molecular weight including associated BF_4^- counterions. [c] Determined from the midpoint of the change in heat capacity. [d] The onset temperature for the decomposition as determined by TGA. [e] The first T_d corresponds to thermolysis of the *tert*-butyl groups.

Table 7. Pyrolytic Conversion of Poly(*tert*-butyl acrylate) Blocks to Poly(acrylic acid)

	M_n (kDa)		weight loss (%)[c]		
polymer	block A[a]	triblock[b]	calcd	exptl	T_d[d,e]
$bpy(PCL\text{-}PtBA)_2$	9.2	32.9	31.4	30.6	195
$bpy(PLA\text{-}PtBA)_2$	29.4	36.6	8.6	6.9	210
$bpy(PS\text{-}PtBA)_2$	6.5	54.3	38.4	39.6	215

[a] Molecular weight determined using MALLS/RI detection in $CHCl_3$. [b] Molecular weights determined by one-shot d*n*/d*c* measurements in which 100% mass recovery from columns was assumed. [c] Percentage weight loss from pyrolysis of the *tert*-butyl esters is calculated from the composition of the polymer as determined by GPC analysis using MALLS. For example, $bpy(PS_n\text{-}PtBA_m)_2$: calcd wt % loss $= [m(MW_{isobutene})/(M_{n,triblock})] \times 100\%$. Experimental wt % loss by TGA = wt % at onset − wt % at offset decomposition temperatures for *tert*-butyl esters. [d] Decomposition temperature for the *tert*-butyl esters to generate isobutene.[39] [e] The decomposition temperature was determined as the onset temperature of first weight loss.

to the decomposition of the *tert*-butyl groups. These data are summarized in Table 7. DSC analysis of $bpy(PCL\text{-}PMMA)_2$ and $bpy(PCL\text{-}PtBA)_2$ exhibited the glass transition temperatures for the outer blocks (PMMA and PtBA); however, the T_g for PCL is out of the range of these experiments (<−20 °C). Block copolymers of PLA with PMMA exhibited only one T_g at ∼90 °C, corresponding to an average of the transitions for the individual polymers. Thermal analysis of the iron-centered star polymers is summarized in Table 6 along with the corresponding macroligand. No significant differences in T_g or T_d were measured for the polymeric metal complexes compared to those of the bipyridine-centered triblocks.

Conclusion

New triblock macroligands have been prepared via ROP and ATRP mechanisms. When combined with metal ions, in this case Fe(II), new metal-centered block copolymer analogues are generated. The iron center in these ordered assemblies could serve as a reactive site that reports on events in the environment, or it can migrate to the surface and become a component of nanoclusters on polymer films. These materials are of interest as templates for nanocluster formation. The presence of tiny, hard inorganic particles on film surfaces can modify interfacial properties. The coordination chemistry of these macroligands with other metal ions, detailed investigation of film properties, and ways in which film morphologies change when stars release their metal ion cores to revert to metal-free triblock macroligands will serve as the subjects of future investigations.

Acknowledgment. We are grateful to the National Science Foundation and to the donors of the Petroleum Research Fund, administered by the American Chemical Society, for support of this work.

References and Notes

(1) Hardy, C. M.; Bates, F. S.; Kim, M.-H.; Wignall, G. D. *Macromolecules* **2002**, *35*, 3189 and references therein.
(2) Fasolka, M. J.; Mayes, A. M. *Annu. Rev. Mater. Res.* **2001**, *31*, 323.
(3) Lee, M.; Cho, B.-K.; Zin, W.-C. *Chem. Rev.* **2001**, *101*, 3869.
(4) Discher, D. E.; Eisenberg, A. *Science* **2002**, *297*, 5583.
(5) Terreau, O.; Luo, L.; Eisenberg, A. *Langmuir* **2003**, *19*, 5601.
(6) Savic, R.; Luo, L.; Eisenberg, A.; Maysinger, D. *Science* **2003**, *300*, 615.
(7) Schubert, U. S.; Eschbaumer, C. *Angew. Chem., Int. Ed.* **2002**, *41*, 2892.
(8) Manners, I. *Science* **2001**, *294*, 1664.
(9) Nguyen, P.; Gomez-Elipe, P.; Manners, I. *Chem. Rev.* **1999**, *99*, 1515.
(10) Bergbreiter, D. E. *Chem. Rev.* **2002**, *102*, 3345.
(11) Gratt, J. A.; Cohen, R. E. *J. Appl. Polym. Sci.* **2003**, *88*, 177.
(12) Cheng, J. Y.; Ross, C. A.; Chan, V. Z.-H.; Thomas, E. L.; Lammertink, R. G. H.; Vansco, G. V. *Adv. Mater.* **2001**, *13*, 1174.
(13) Ahmed, S. R.; Kofinas, P. *Macromolecules* **2002**, *35*, 3338.
(14) Kokanyan, E. P.; Babajanyan, V. G.; Demirkhanyan, G. G.; Gruber, J. B.; Erdei, S. *J. Appl. Phys.* **2002**, *92*, 1544.
(15) Torchilin, V. P. *Adv. Drug Deliv. Rev.* **2002**, *54*, 235.
(16) Wiessleder, R.; Bogdanov, A.; Tung, C.-H.; Weinmann, H.-J. *Bioconjugate Chem.* **2001**, *12*, 213.
(17) Caravan, P.; Ellison, J. J.; McMurry, T. J.; Lauffer, R. B. *Chem. Rev.* **1999**, *99*, 2293.
(18) Temple, K.; Kulbaba, K.; Power-Billard, K. N.; Manners, I.; Leach, K. A.; Xu, T.; Russell, T. P.; Hawker, C. J. *Adv. Mater.* **2003**, *15*, 297.
(19) Raez, J.; Zhang, Y.; Cao, L.; Petrov, S.; Erlacher, K.; Wiesner, U.; Manners, I.; Winnik, M. A. *J. Am. Chem. Soc.* **2003**, *125*, 6010.
(20) Boontongkong, Y.; Cohen, R. E.; Rubner, M. F. *Chem. Mater.* **2000**, *12*, 1628.
(21) Wang, T. C.; Rubner, M. F.; Cohen, R. E. *Chem. Mater.* **2003**, *15*, 299.
(22) Wolf, J. H.; Hillmyer, M. A. *Langmuir* **2003**, *19*, 6553.
(23) Shin, K.; Leach, K. A.; Goldbach, J. T.; Kim, D. H.; Jho, J. Y.; Tuominen, M.; Hawker, C. J.; Russell, T. P. *Nano Lett.* **2002**, *2*, 933.
(24) Spatz, J. P.; Chan, V. Z.-H.; Mö*β*mer, Kamm, F.-M.; Plettl, A.; Ziemann, P.; Möller, M. *Adv. Mater.* **2002**, *14*, 1827.
(25) Haupt, M.; Miller, S.; Roman, G.; Arnold, M.; Sauer, R.; Thonke, K.; Möller, M.; Spatz, J. P. *Adv. Mater.* **2003**, *15*, 16.
(26) Park, C.; McAlvin, J. E.; Fraser, C. L.; Thomas, E. L. *Chem. Mater.* **2002**, *14*, 1225.
(27) Smith, A. P.; Corbin, P. S.; Fraser, C. L. *Tetrahedron Lett.* **2000**, *41*, 2787.
(28) Keller, R. N.; Wycoff, H. D. *Inorg. Synth.* **1946**, *2*, 1.
(29) Pangborn, A. B.; Giardello, M. A.; Grubbs, R. H.; Rosen, R. K.; Timmers, F. J. *Organometallics* **1996**, *15*, 1518.
(30) The estimated chelation efficiency (CE): $\epsilon_{MLCT}[Fe(bpyX_2)_3]^{2+}/\epsilon_{MLCT}[Fe(bpy)_3]^{2+}$. $\lambda_{max}[Fe(bpy)_3]^{2+}$ in 3:1 CH_2Cl_2/CH_3OH = 522 nm, and ϵ = 9450 M^{-1} cm^{-1}.
(31) Corbin, P. S.; Webb, M. P.; McAlvin, J. E.; Fraser, C. L. *Biomacromolecules* **2001**, *2*, 223.
(32) Matyjaszewski, K.; Xia, J. *Chem. Rev.* **2001**, *101*, 2921.
(33) Xia, J.; Matyjaszewski, K. *Macromolecules* **1997**, *30*, 7697.
(34) Ma, Q.; Wooley, K. L. *J. Polym. Sci., Part A: Polym. Chem.* **2000**, *38*, 4805.
(35) Davis, K. A.; Matyjaszewski, K. *Macromolecules* **2000**, *33*, 4039.
(36) Wu, X.; Fraser, C. L. *Macromolecules* **2000**, *33*, 4053.
(37) Uegaki, H.; Kotani, Y.; Kamigaito, M.; Sawamoto, M. *Macromolecules* **1998**, *31*, 6756.
(38) Johnson, R. M.; Corbin, P. S.; Ng, C.; Fraser, C. L. *Macromolecules* **2000**, *33*, 7404.
(39) Zhang, Q.; Remsen, E. E.; Wooley, K. L. *J. Am. Chem. Soc.* **2000**, *122*, 3642.

(40) McAlvin, J. E.; Scott, S. B.; Fraser. C. L. *Macromolecules* **2000**, *33*, 6953.
(41) Wu, X.; Fraser, C. L. *Macromolecules* **2000**, *33*, 4053.
(42) Seo, Y.; Esker, A. R.; Sohn, D.; Kim, H.-J.; Park, S.; Yu, H. *Langmuir* **2003**, *19*, 3313.
(43) Rharbi, Y.; Winnik, M. A. *Macromolecules* **2001**, *34*, 5238.
(44) Guo, Y.-M.; Pan, C.-Y.; Wang, J. *J. Polym. Sci., Part A: Polym. Chem.* **2001**, *39*, 2134.
(45) Glauser, T.; Stancik, C. M.; Möller, M.; Voytek, S.; Gast, A. P.; Hedrick, J. L. *Macromolecules* **2002**, *35*, 5774.
(46) Meyer, U.; Palmans, A. R. A.; Loontjens, T.; Heise, A. *Macromolecules* **2002**, *35*, 2873.
(47) Smith, A. P.; Fraser, C. L. *Macromolecules* **2003**, *36*, 2654.
(48) Smith, A. P.; Fraser, C. L. *J. Polym. Sci., Part A: Polym. Chem.* **2002**, *40*, 4250.
(49) Kamigaito, M. Ando, T.; Sawamoto, M. *Chem. Rev.* **2001**, *101*, 3689.
(50) Matyjaszewski, K.; Shipp, D. A.; Wang, J.-L.; Grimaud, T.; Patten, T. E. *Macromolecules* **1998**, *31*, 6836.
(51) Fraser, C. L.; Smith, A. P. *J. Polym. Sci., Part A: Polym. Chem.* **2000**, *38*, 4704.
(52) Davis, K. A.; Matyjaszewski, K. *Macromolecules* **2001**, *34*, 2101.
(53) Eastwood, E. A.; Dadmun, M. D. *Macromolecules* **2001**, *34*, 740.
(54) Wang, X.-S.; Luo, N.; Ying, S.-K. *Polymer* **1999**, *40*, 4157.
(55) Gold, L. *J. Chem. Phys.* **1958**, *28*, 91.
(56) Wu, X.; Fraser, C. L. *Macromolecules* **2000**, *33*, 4053.
(57) Davis, K. A.; Charleux, B.; Matyjaszewski, K. *J. Polym. Sci., Part A: Polym. Chem.* **2000**, *38*, 2274.
(58) Burguière, C.; Pascual, S.; Bui, C.; Vairon, J.-P.; Charleux, B.; Davis, K. A.; Matyjaszewski, K.; Bétremieux, I. *Macromolecules* **2001**, *34*, 4439.
(59) Johnson, R. M.; Fraser, C. L. Manuscript in preparation.
(60) Johnson, R. M.; Fraser, C. L. Manuscript submitted.

MA035494+